EXPRESSION, PURIFICATION, AND KINETIC CHARACTERIZATION OF HUMAN LIVER PHOSPHOFRUCTOKINASE

A Thesis

by

AMANDA JEAN TINDALL

Submitted to the Office of Graduate and Professional Studies of
Texas A&M University
in partial fulfillment of the requirements for the degree of

MASTER OF SCIENCE

Chair of Committee,	Gregory D. Reinhart
Committee Members,	Jennifer K. Herman
	J. Martin Scholtz
	Hays S. Rye
Head of Department,	Gregory D. Reinhart

May 2016

Major Subject: Biochemistry

ABSTRACT

Phosphofructokinase (PFK) catalyzes the phosphorylation of fructose 6-phosphate (F6P) to fructose 1,6-bisphosphate (F16BP) in a MgATP dependent reaction. This reaction represents the first committed step of the glycolytic pathway and as such, plays an important role in metabolism. In liver, this regulation is especially interesting, as hepatocytes can alternatively undergo gluconeogenesis or glycolysis. While PFKs from the livers of several mammalian species have been characterized, human liver PFK has not been thoroughly examined. The gene encoding human liver PFK was cloned into an expression vector utilizing the *tac* promoter. Human liver PFK was expressed in an *Escherichia coli* strain, RL257a, which contains no native PFK. The protein has been purified to a specific activity of 130 U/mg through a combination of heat denaturation, ammonium sulfate precipitation, anion exchange chromatography, and gel filtration chromatography. Human liver PFK is inhibited by MgATP with a coupling free energy (ΔG_{ax}) of 3.0 kcal/mol, as compared to rat liver PFK (ΔG_{ax} 2.3 kcal/mol), a well characterized mammalian PFK. Additionally, human liver PFK demonstrates greater than 10-fold increase in F6P affinity when the pH is increased as demonstrated by the dissociation constants at pH 6 (K_{ia} 0.70) and pH 9 (K_{ia} 0.032). At the cellular concentration of 3 mM MgATP, F16BP activates the enzyme (ΔG_{ax} -0.69 kcal/mol), while citrate inhibits the enzyme (ΔG_{ax} 0.62 kcal/mol). The additional activators ammonium sulfate (ΔG_{ax} -2.0 kcal/mol) and AMP also impact the activity of HLPFK. These results suggest that the human liver enzyme is less sensitive to allosteric effectors than the rat liver enzyme, with the possible exception of MgATP.

DEDICATION

to my dad, Don Tindall, for his love of science

ACKNOWLEDGEMENTS

I would like to thank my advisor, Dr. Gregory D. Reinhart, for his guidance over the course of my graduate work. Thanks go to the members of my committee, who have been quick to offer advice, especially Dr. Jennifer Herman. The members of the Biochemistry and Biophysics department have helped me in ways too numerous to mention during my time here. The past and present members of the Reinhart lab have made hr in the lab enjoyable. David Holland deserves special thanks because of his helpful suggestions throughout my work with the human enzyme and his donation of rat liver phosphofructokinase. Special thanks go to Robert Koenig for his patient support, and to our families for their encouraging words.

TABLE OF CONTENTS

LIST OF FIGURES

LIST OF TABLES

CHAPTER I

INTRODUCTION

Phosphofructokinase (PFK) catalyzes the first committed step of the glycolytic pathway and, as such, plays an important role in glucose metabolism. PFK transfers the γ-phosphate group of adenosine triphosphate (ATP) to fructose-6-phosphate (F6P) to form fructose-1,6-bisphosphate (F16BP) and adenosine diphosphate (ADP). An accurate picture of glucose metabolism regulation is critical to understanding a number of diseases, including some cancers,[1–5] diabetes,[6,7] Tarui disease,[8] and Down's Syndrome.[9,10]

PFK is present in both prokaryotic and eukaryotic cells. Prokaryotic PFKs have been studied from a wide variety of organisms for many years. In general, they are activated by MgADP and inhibited by phosphoenolpyruvate (PEP), which both act as K-type allosteric effectors; that is, they modify substrate affinity without affecting the maximal velocity of PFK. Eukaryotic PFK investigations have focused on the enzyme from *Saccharomyces* sp. or from mammalian tissues. In mammals, three isoforms of PFK are differentially present in a tissue-specific manner. These three isozymes have been identified as: PFK-L (liver), PFK-M (muscle), and PFK-C (platelet).[11–16] These isozymes associate into homo and heterotetramers in a tissue specific fashion. In liver, PFK predominantly forms a homotetramer of L-type subunits although PFK-M and PFK-C are also present.[11,14–16]

As a key control point in the glycolytic pathway, mammalian PFK activity is regulated by a variety of cellular effectors and by self-association to form higher order oligomers.[17–21] As a prerequisite to understanding cellular regulation, it is important to

measure the physiological concentrations of relevant molecules, including substrates, products, and allosteric effectors. PFK in hepatocytes is present at 20-50 μg/mL[17] and the intracellular concentrations of several effectors, ATP (3 mM[20,22]), F6P (0.02 mM-0.06 mM[20,22]), AMP (0.3 mM[23]), F16BP (20 μM[22]), citrate (0.2 mM[24]), and ammonia (0.6 mM[25]), modify PFK activity.[24]

The study of specific mammalian PFKs began with the purification of rabbit muscle by the Lardy group.[26] They purified PFK from rabbit muscle tissues and completed initial kinetic studies, in addition to identifying the stabilizing effect of MgATP on purified rabbit muscle PFK. Additional groups studied PFKs from a variety of sources, as reviewed by Uyeda in 1979[27] and recently by Schöneberg[28] and Sola-Penna.[29] These reviews summarize purification, regulation, mechanism, and structures of both eukaryotic and prokaryotic PFKs.

Rabbit muscle PFK is inhibited by a substrate, ATP, at a second binding site and activated by products, ADP and F16BP. Additionally, citrate and lactate inhibit while AMP, cAMP, F26BP, and acetyl CoA activate rabbit muscle PFK.[29–32] These molecules all represent cellular indicators of metabolic needs. In addition to direct regulation by metabolites, it has been demonstrated that these molecules can modify the quaternary structure of the enzyme.[17–20] ATP, citrate, and lactate (in muscle, but not liver) interact with PFK in a manner that favors dissociation of the tetramer and diminishes PFK activity when cellular energy levels are high. ADP, F6P, and AMP favor association of the tetramer, allowing for increased PFK activity under energy-poor conditions. While muscle PFK shares a 68.6% amino acid sequence identity with liver PFK, the regulation of muscle

PFK is different than liver PFK. While both muscle and liver can PFKs self-associate, the concentration of PFK in muscle (0.45-2 mg/g[33]) is much higher than in liver (12-30 µg/g[17]) leading to different association behavior between the PFK isoforms present in specific tissue types. The understanding of higher order structures is convenient for the development of purification technique with a notable example of active higher-order oligomers being exploited during the purification of RLPFK. Reinhart[24] demonstrated that in the presence of F6P, RLPFK elutes from a Sepharose 2B column in the void volume, indicating a molecular weight greater than 40,000 kD. This allowed for efficient separation from smaller molecules.

In addition to direct effects by metabolites and quaternary structure, liver PFK activity is indirectly modified by the action of the hormone glucagon[34–37] through the presence of glucagon receptors on the surface of the hepatocytes. Glucagon binds to receptors and activates a signal transduction pathway utilizing a G protein which in turn activates adenylate cyclase. Adenylate cyclase generates cAMP which then caused protein kinase A to phosphorylate phosphofructokinase-2/fructose 2,6-bisphosphatase. The phosphorylation activates the fructose 2,6-bisphosphatase domain, which degrades intracellular fructose-2,6-bisphosphate (F26BP), leading to a decrease in glycolysis through reduction of activation of PFK. Fructose-2,6-bisphosphate is a potent allosteric activator of liver PFKs[38–42] and plays a critical role in liver PFK accurately responding to cellular energetic needs.

Structural studies of mammalian PFKs have included electron microscopy and crystallography, among other techniques. Electron micrographs of human muscle PFK

showed tetramers at 18Å resolution.[43] Rabbit muscle PFK has formed crystals which have diffracted with increasing resolution, the most recent of which was published in 2011 with a resolution of 3.2Å (3O8L),[44] while human muscle PFK was crystallized in 2014 and the structure determined at 6.0Å (4OMT).[45] Human PFK-C has also been crystallized, with and without ligands, by Kloos *et al* (4XZ2)[46] and Webb *et al* (4XYK),[47] both in 2015. The structure of liver PFK has remained elusive for structural biochemists, possibly due to the formation of undefined higher order oligomers.[21,48,49] The published structures have presented a homodimer, half of the physiological homotetramer, in addition to identifying some of the ligand binding sites.

The gene for human liver phosphofructokinase was identified as part of chromosome 21[50] with the cDNA sequence published in 1989.[51] Initial investigations focused on identification of tissues expressing HLPFK. The molecular weight of each human PFK-L subunit was determined to be 85kD.[16] While human muscle PFK has been expressed and crystallized,[45] there is minimal kinetic data available for human liver PFK. This work seeks to provide new data regarding the expression, purification, and characterization of human liver phosphofructokinase.

CHAPTER II

MATERIALS AND METHODS

Materials

The gene for HLPFK was ordered from Biomatik, Cambridge, ON, based on the amino acid sequence of HLPFK shown in Figure 1. The company used proprietary methods to synthesize codon-optimized *hlpfk* for expression in *Escherichia coli* cells. The pUC19 plasmid was purchased from New England Biolabs and the pALTER-EX1 plasmid was purchased from Promega. The *E. coli* strain, RL257a, is a *tonA*$^{-}$ derivative of RL257.[52] Reagents and kits for molecular biology techniques were from New England Biolabs and Qiagen.

```
MAAVDLEKLR ASGAGKAIGV LTSGGDAQGM NAAVRAVTRM GIYVGAKVFL IYEGYEGLVE
GGENIKQANW LSVSNIIQLG GTIIGSARCK AFTTREGRRA AAYNLVQHGI TNLCVIGGDG
SLTGANIFRS EWGSLLEELV AEGKISETTA RTYSHLNIAG LVGSIDNDFC GTDMTIGTDS
ALHRIMEVID AITTTAQSHQ RTFVLEVMGR HCGYLALVSA LASGADWLFI PEAPPEDGWE
NFMCERLGET RSRGSRLNII IIAEGAIDRN GKPISSSYVK DLVVQRLGFD TRVTVLGHVQ
RGGTPSAFDR ILSSKMGMEA VMALLEATPD TPACVVTLSG NQSVRLPLME CVQMTKEVQK
AMDDKRFDEA TQLRGGSFEN NWNIYKLLAH QKPPKEKSNF SLAILNVGAP AAGMNAAVRS
AVRTGISHGH TVYVVHDGFE GLAKGQVQEV GWHDVAGWLG RGGSMLGTKR TLPKGQLESI
VENIRIYGIH ALLVVGGFEA YEGVLQLVEA RGRYEELCIV MCVIPATISN NVPGTDFSLG
SDTAVNAAME SCDRIKQSAS GTKRRVFIVE TMGGYCGYLA TVTGIAVGAD AAYVFEDPFN
IHDLKVNVEH MTEKMKTDIQ RGLVLRNEKC HDYYTTEFLY NLYSSEGKGV FDCRTNVLGH
LQQGGAPTPF DRNYGTKLGV KAMLWLSEKL REVYRKGRVF ANAPDSACVI GLKKKAVAFS
PVTELKKDTD FEHRMPREQW WLSLRLMLKM LAQYRISMAA YVSGELEHVT RRTLSMDKGF
```

Figure 1: Primary Sequence of HLPFK.

Reagents and enzymes were from the following sources: ATP, AMP, F6P, and F16BP (sodium salts), DTT, aldolase and triose phosphate isomerase (ammonium sulfate

suspensions), MOPS, TRIS base, CHES, MES, and citric acid, Sigma-Aldrich; Luria-Bertani media (Miller), BD Bioscience; NADH, and tetracycline, Research Products International Corp.; IPTG, Fisher Scientific; glycerol-3-phosphate dehydrogenase, lactate dehydrogenase, and pyruvate kinase (ammonium sulfate suspensions), PEP (monopotassium salt), Roche; MonoQ, HiQ, and Sepharose 2B resins, Pharmacia (now GE Healthcare); Reducing Agent Compatible Pierce BCA Protein Assay Kit, ThermoFisher; All chemicals and reagents were of the highest purity available. Deionized, distilled water was used for all experiments.

Molecular Biology

The *hlpfk* gene was initially supplied in a pUC19 plasmid. The plasmid was digested using *BamHI* and *EcoRI* and subject to electrophoresis on a 1% agarose gel. The gel containing the *hlpfk* gene was extracted and the DNA was purified using the QIAquick Gel Extraction Kit. The pALTER-EX1 plasmid was similarly digested, although not subject to electrophoresis. The *hlpfk* gene was ligated into the vector using T4 DNA Ligase at room temperature overnight. The ligated sample was heat inactivated at 65°C for 10 min and transformed into chemically competent (calcium treated) JM109 *E. coli* cells. Transformants were grown at 37°C overnight. The plasmids from selected colonies were sequenced by Eton Sequencing to confirm construction.

The addition of the ribosome binding site to the plasmid for enhanced cellular expression of *hlpfk* began with the design of primers. Primers were chosen to amplify the gene from the initial pALTER-EX1 construct. Figure 2 contains the primers constructed for polymerase chain reaction (PCR) amplification. The gene was amplified using

PhusionHF Polymerase. The thermal cycle was programmed for 10s at 98°C for initial denaturation, followed by 34 cycles of 10s at 98°C for denaturation, 30s at 56°C for annealing, 90s at 72°C for extension, and 10 min at 72°C for the final extension. The resulting PCR amplicons were cleaned up using a QIAquick PCR Purification Kit and then digested with *BamHI* and *EcoRI* for 2 hr at 37°C. The pALTER-EX1 plasmid was also digested with *BamHI* and *EcoRI*. After digestion, both vector and amplicon were cleaned with the QIAquick PCR Purification Kit and treated with Antarctic Phosphatase. After another pass through the QIAquick PCR Purification Kit, the amplicon was ligated into the vector using T4 DNA Ligase at room temperature for two hours. The ligated sample was heat inactivated, transformed into JM109 *E. coli* cells, grown, and sequenced as above.

Forward: 5' GTACAGGATCC**TAAGGAGG**CAGGAAAC **ATG GCA GCG GTT GAC CTG G** 3'

Reverse: 5' GTACAGAATTC**ATTA GAA ACC TTT GTC CAT AGA C** 3'

Figure 2: Primer Construction. Underlined bases represent restriction enzyme sites (BamHI forward, EcoRI reverse). The red bases are the optimized ribosome binding site, and the bolded bases represent the *hlpfk* gene.

Kinetic Analysis

Maximal velocity enzyme assays were performed in a cuvette containing 0.6 mL of reaction mixture (50 mM Tris-HCl pH 8.5, 100 mM KCl, 0.1 mM EDTA, 20 mM $(NH_4)_2SO_4$, 5 mM DTT, 400 µg aldolase, 40 µg triose phosphate isomerase, and 40 µg glycerol-3-phosphate dehydrogenase). The coupling enzymes, aldolase, triose phosphate

isomerase, and glycerol-3-phosphate dehydrogenase, are present to oxidize NADH and to prevent F16BP accumulation. Therefore consumption of F6P is coupled to change in absorbance at 340nm by a two-fold turnover of NADH to NAD^+ as shown in Figure 3A. This assay allows for increased sensitivity to PFK activity.

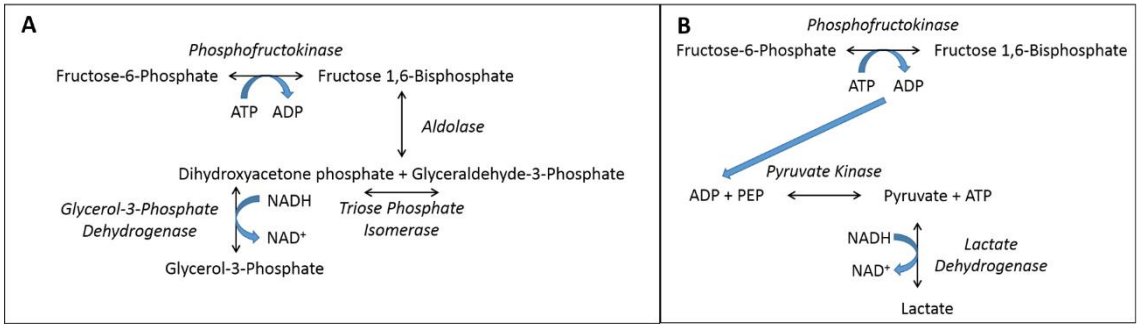

Figure 3: Coupled Assay Systems. (A) represents the coupling enzymes used in all assays except those examining F16BP while (B) represents the coupling enzyme system used to examine the effect of F16BP.

The allosteric properties of the enzyme were investigated in a cuvette containing 0.6 mL of the reaction mixture (50 mM MOPS-KOH pH 7.0, 100 mM KCl, 0.1 mM EDTA, 5 mM DTT, 5 mM $MgCl_2$, 400 µg aldolase, 40 µg triose phosphate isomerase, and 40 µg glycerol-3-phosphate dehydrogenase). MgATP, F6P, and allosteric effectors are varied as indicated. For experiments studying the effect of pH on HLPFK, MES-KOH (pK_a 6.1) at pH 6.0, Tris-HCl (pK_a 8.1) at pH 8.0, or CHES-KOH (pK_a 9.5) at pH 9.0 was substituted for MOPS-KOH.

In order to study the effect of F16BP, it is necessary to use alternate coupling enzymes, pyruvate kinase and lactate dehydrogenase, and 1 mM PEP as shown in Figure

3B. When the total formation of F16BP is very low (<10 μM), this system allows for analysis of the coupling between F6P and F16BP at different MgATP concentrations. While the aldolase, triose phosphate isomerase, and glycerol-3-phosphate dehydrogenase system generates two NAD^+ molecules for each F6P molecule consumed, the pyruvate kinase and lactate dehydrogenase system generates one NAD^+ molecule.

All assays conducted in this work were completed on a Beckman Series 600 spectrophotometer at 25°C. Coupling enzymes were desalted prior to use by extensive dialysis against the experimental buffer to remove ammonium sulfate. From the coupled assay conditions, the change in absorbance is related to the change in substrate concentration as related by Beer's Law (ε_{NADH} 6.22 mM^{-1} cm^{-1}). By limiting the substrate to a total decrease of less than 10%, the assay measures the initial rate under steady state conditions. The measurement of initial rates at low substrate concentrations allows for more accurate rate determinations.

The initial rates, reported as specific activity (Units/mg protein, where one unit represents 1μmol F16BP or ADP per minute), are plotted as a function of substrate concentration and fit to the Hill equation (Equation 1) to determine $K_{1/2}$ under rapid equilibrium conditions. Fitting data to Equation 1 using different concentrations of effectors provides the basis to calculate the coupling between two ligands. Figure 4 illustrates the shift in the graph when the effector is an activator (A) or an inhibitor (B).

$$v_0 = \frac{V_{max}[S]^n}{K_{1/2}^n + [S]^n} \quad (1)$$

After initial rate data is fit to the Hill equation, the $K_{1/2}$ values are plotted as a function of effector. In order to quantify the allosteric effect of a ligand, the

thermodynamic linkage analysis of protein-ligand interactions initially described by Weber[53] serves as a basis for extended analysis used by Reinhart.[54–56]

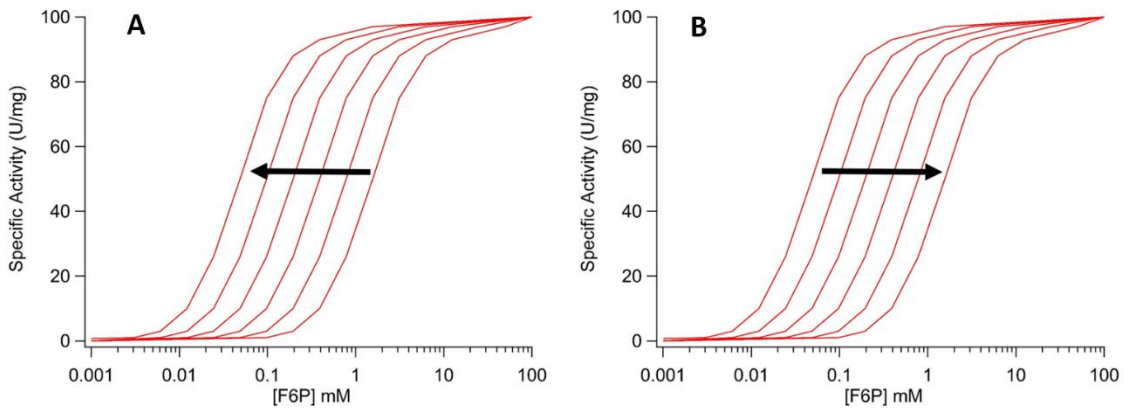

Figure 4: Simulated $K_{1/2}$ Shifts with Allosteric Effector. (A) represents the $K_{1/2}$ shift for an activator while (B) demonstrates the $K_{1/2}$ shift for an inhibitor.

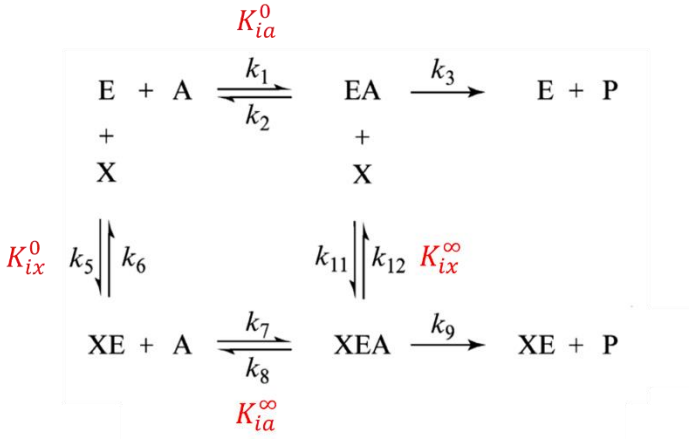

Figure 5: Single Substrate, Single Modifier Scheme. The dissociation constants defined in the text are indicated in red beside the relevant rate constants.

The linkage model suggests four enzyme forms shown in Figure 5: E (free enzyme), EA (enzyme with substrate), XE (enzyme with allosteric effector), and XEA (enzyme with both substrate and allosteric effector). From the kinetic rate constants, we can define thermodynamic dissociation constants: $K_{ia}^{0}=\frac{k_2}{k_1}$, $K_{ia}^{\infty}=\frac{k_8}{k_7}$, $K_{ix}^{0}=\frac{k_6}{k_5}$, and $K_{ix}^{\infty}=\frac{k_{12}}{k_{11}}$ where the superscript '0' indicates the absence of the second ligand and the superscript '∞' indicates saturation with the second ligand. From these dissociation constants we can quantify the magnitude of the allosteric effect by defining the coupling quotient:

$$Q_{ax} = \frac{K_{ia}^{0}}{K_{ia}^{\infty}} = \frac{K_{ix}^{0}}{K_{ix}^{\infty}} \tag{2}$$

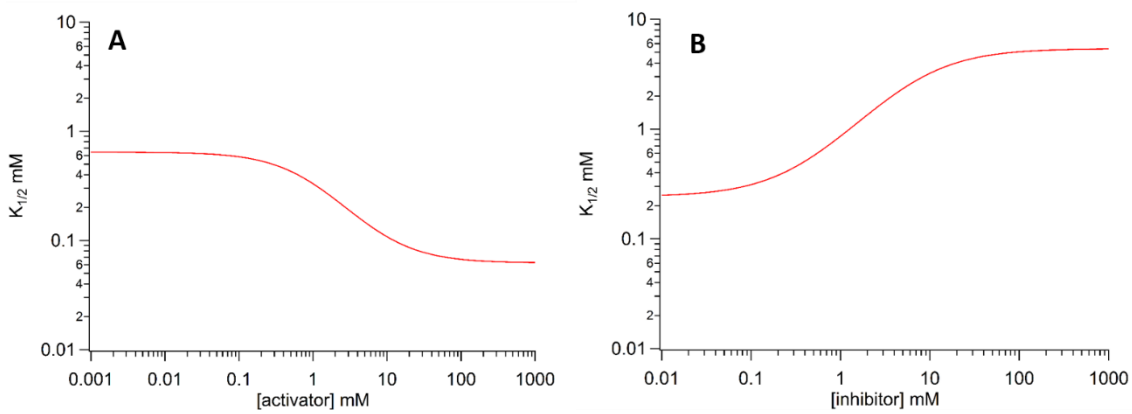

Figure 6: Simulated Coupling. An activator is represented in (A) while an inhibitor is represented in (B).

When the rapid equilibrium assumption is valid, $K_{1/2}$ can be plotted as a function of effector. Graphically, the coupling quotient is equal to the ratio of the bottom to top

plateaus, shown in Figure 6. When the coupling quotient is equal to 1, there is no allosteric effect. For values less than 1, the allosteric effector acts as an inhibitor while values greater than 1 indicate an allosteric activator. When $K_{1/2}$ is plotted as a function of effector concentration (X), the data are described by Equation 3:

$$K_{1/2} = K_{ia}^{0} \frac{K_{ix}^{0} + X}{K_{ix}^{0} + Q_{ax}(X)} \quad (3)$$

Determination of the coupling quotient (Q_{ax}) allows calculation of the coupling free energy based on the relationships shown in Equation 5:

$$\Delta G_{ax} = -RT \ln Q_{ax} \quad (4)$$

When the rapid equilibrium assumption is valid and steady state rates are measured, Q_{ax} represents the equilibrium constant for the disproportionate equilibrium shown in Equation 5. This analysis calculates thermodynamic parameters from kinetic measurements, setting the stage for simple comparisons across multiple systems.

$$EA + XE \overset{Q_{ax}}{\longleftrightarrow} XEA + E \quad (5)$$

CHAPTER III

RESULTS

Growth and Expression

In order to begin studying HLPFK, the first step was to determine a successful expression and purification procedure. Using the amino acid sequence in Figure 1, the *E. coli* codon-optimized *hlpfk* was ordered from Biomatik. The synthesized cDNA was initially located in a pUC19 plasmid; upon arrival, the gene was cloned into pALTER-EX1. The pALTER-EX1 plasmid contains tet^r, which permits growth in tetracycline; expression is controlled by the *tac* promoter and *hlpfk* is inducible with isopropyl β-D-1-thiogalactopyranoside (IPTG). The protein was expressed in a derivative of RL257,[52] with the *tonA* gene knocked out to prevent infection by phage.

Early preps expressed little HLPFK, despite different growth temperatures (37°C, 30°C, or some combination thereof), different growth times, and different concentrations of IPTG. Based on the suggestion of Dr. Jennifer Herman, an optimized ribosome binding site (RBS), TAAGGAGG,[57] was substituted for the RBS already present (AGGA). As shown in Table 1, the addition of the optimized RBS increased the expression by almost five-fold.

Cells were grown under selective pressure by tetracycline by inoculating 6 L of Luria-Bertani media (Miller) with 6 mL of an overnight culture grown to stationary phase (also with tetracycline). Cultures were incubated at 30°C while shaking at 250 rotations per minute until an optical density of 0.6 at 600 nm is reached; then they are induced with

1 mM IPTG and incubated at 30°C while shaking at 250 rpm for a total growth time of 30 hr. This growth typically yields approximately 20g wet weight of cells with about 450U/g.

Table 1: HLPFK Expression.

	Total Units (U)	Wet Weight of Cells (g)	U/g
HLPFK	814	7.45	109
HLPFK + RBS	2910	6.25	465

Purification

As the challenges in expression were investigated, two similar purifications that both yielded purified HLPFK were developed. Both purification protocols were adapted from previous work with RLPFK.[24] The major differences lie in the initial purification buffer (Purification I used a phosphate buffer with F6P while Purification II used a tris buffer with ATP), the ammonium sulfate procedure (Purification I fractionates with ammonium sulfate while Purification II continues with proteins that precipitate at 33%), and the anion exchange protocol and buffers (Purification I used a MonoQ resin with a higher ionic strength buffer while Purification II used a HiQ resin and lower ionic strength buffer). Purification I yielded a protein with a specific activity of 105 U/mg while Purification II yielded a sample with a specific activity of 130 U/mg. HLPFK requires F6P or MgATP in all buffers to maintain activity.

Purification I

Cells were resuspended in purification buffer (20 mM KP_i pH 7.6, 3 mM $MgSO_4$, 5 mM DTT, 0.1 mM EDTA, 1 mM F6P) with 1 mM phenylmethanesulfonyl fluoride (PMSF), then sonicated to lyse cells. Sonication was completed by pulsing for 15 sec and resting for 45 sec for a total pulse time of 10 min. The crude lysate was centrifuged for 30 min at 20000 *g* at 4°C. The sonication typically yields a crude lysate with a specific activity of 0.63 U/mg.

The supernatant was then heated to 55±1°C for 3 min by slowly swirling the solution in a flask immersed intermittently in a boiling water bath. After the heat denaturation, the solution was rapidly cooled to less than 10°C by swirling the flask in an ice-water bath. The heat denatured lysate was centrifuged for 30 min at 20000 *g* at 4°C and the supernatant generally has a specific activity of 1.3 U/mg. The heat denatured supernatant was then fractionated with ammonium sulfate. Ammonium sulfate was added to supernatant slowly, while stirring on ice, and then the entire solution was maintained at 4°C for 90 min without stirring. Pellets were harvested by centrifugation for 20 min at 9000 *g* at 4°C. The greatest activity was found in the pellet containing proteins precipitated between 45% and 50% ammonium sulfate. The resuspension of that pellet yielded a specific activity of 11 U/mg.

The precipitated proteins are dialyzed against the column buffer A (50 mM Tris-HCl pH 8.0, 100 mM KCl, 20 mM $(NH_4)_2SO_4$, 5 mM DTT, 0.1 mM EDTA, 3 mM $MgCl_2$, 1 mM F6P), then diluted to about 1 mg/mL and loaded to a pre-equilibrated MonoQ anion exchange column. The column was washed with column buffer A, then proteins were

eluted with a gradient of column buffer B, which is the same as column buffer A with the addition of 1 M NaCl. The NaCl gradient has three steps, the first from 0-10%, the second from 10-25%, and the third step from 25-100%. Fractions were assayed for activity and selectively pooled to generate the highest specific activity. Figure 7A shows the elution profile from the MonoQ. The pooled fractions had a specific activity of 22 U/mg.

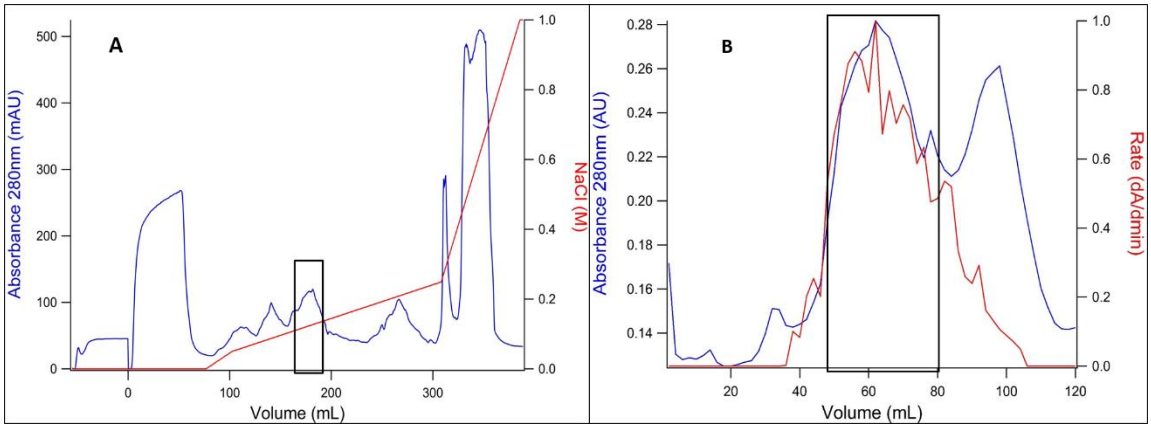

Figure 7: Elution Profiles of Purification I. (A) MonoQ elution profile where protein is indicated by the absorbance at 280 nm shown in blue. The red line indicates the molarity of NaCl and the black box represents the pooled fractions. (B) Sepharose 2B elution profile where protein is indicated by the absorbance at 280 nm (blue) and the activity of the sample is shown in red. The black box indicates pool.

The sample was concentrated with 55% ammonium sulfate and resuspended to a volume of about 2 mLs in purification buffer, then loaded to a 344 mL (1.7 cm x 38.6 cm) Sepharose 2B column and eluted with purification buffer. Fractions were again assayed for activity and selectively pooled for purity. Purified protein was dialyzed into and then maintained in storage buffer (20 mM KP_i pH 7.6, 3 mM $MgSO_4$, 5 mM DTT, 0.1 mM

EDTA, 1 mM F6P, and 20% glycerol (w/v)) for up to two months before activity decreased. Figure 7B shows the elution profile from the gel filtration.

Protein concentration was determined for each sample by precipitating protein with 20% trichloroacetic acid and then using the Pierce BCA Assay Kit. Purity was evaluated by SDS-PAGE. Figure 8 is a 10% SDS PAGE gel showing the purity of each purification step and the final product. The purification steps are summarized in Table 2.

Table 2: Summary of HLPFK Purification I.

Sample	Vol (mL)	Activity (U/mL)	Protein (mg/mL)	Specific Activity (U/mg)	Total Units (U)	Yield (%)	Purification Fold
Cleared Lysate	96	12	20	0.63	1190	100	1
Heat Denaturation	90	14	11	1.3	1260	106	2
$(NH_4)_2SO_4$ Precipitate	13	46	4.2	11	580	49	18
MonoQ	32	20	0.90	22	633	53	35
Sepharose 2B	2.8	72	0.70	105	201	17	167

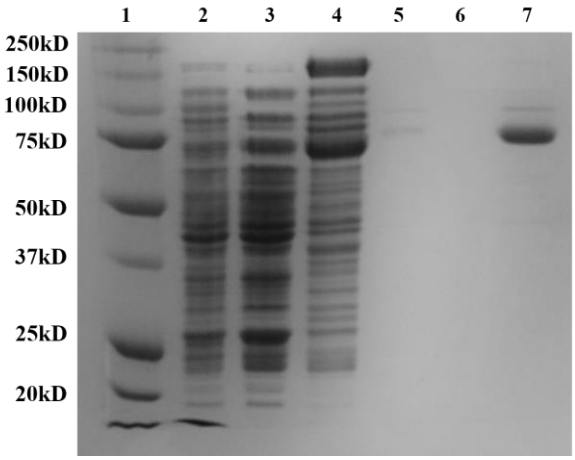

Figure 8: SDS-PAGE of Purification I. The lanes of this 10% SDS-PAGE show (1) molecular weight marker, (2) cleared lysate, (3) heat denaturation, (4) ammonium sulfate precipitate, (5) dilute MonoQ pool, (6) empty, and (7) purified HLPFK.

Purification II

Cells were resuspended in buffer (50 mM Tris-HCl pH 8, 50 mM NaF, 1 mM ATP, and 5 mM DTT) with 1 mM PMSF, then sonicated and centrifuged, as in Purification I. The sonication typically yielded a crude lysate with a specific activity of 4.4 U/mg. The crude lysate was then heat denatured as in Purification II to generate supernatant with a specific activity of 8.7 U/mg, which was then precipitated with 33% ammonium sulfate. Ammonium sulfate was added to supernatant slowly, while stirring on ice, and then the entire solution was maintained at 4°C for 90 min without stirring. The pellet was harvested by centrifugation for 20 min at 9000 *g* at 4°C and the resuspended pellet yielded a specific activity of 25 U/mg.

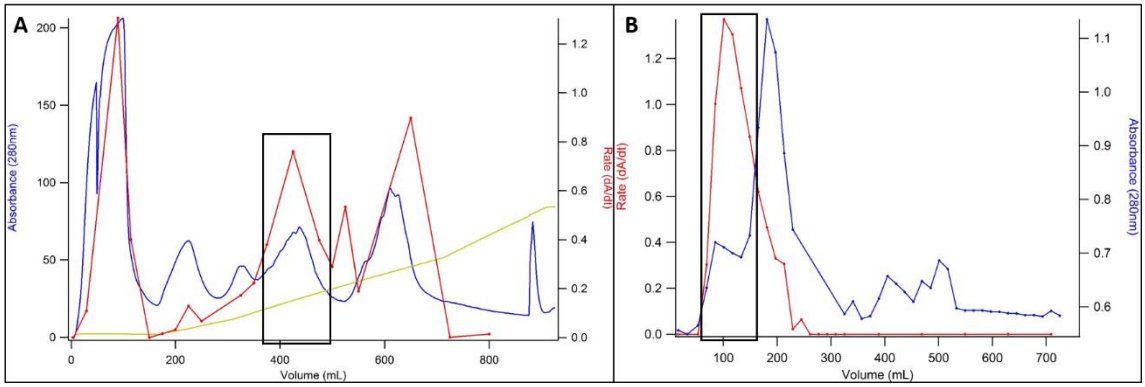

Figure 9: Elution Profiles of Purification II. (A) HiQ elution profile with absorbance at 280nm in blue, activity in red, NaCl gradient in yellow, and pooled fractions indicated by the black box. (B) Sepharose 2B elution profile with absorbance at 280nm in blue, enzyme activity in red, and the black box indicates pooled fractions.

The precipitated proteins were dialyzed against a modified column buffer A from that used in Purification I (50 mM Tris-HCl pH 8.0, 5 mM DTT, 0.1 mM EDTA, 5 mM

$MgCl_2$, 1 mM F6P, and 0.02% NaN_3), then diluted to about 1 mg/mL and loaded to a pre-equilibrated HiQ anion exchange column. The column was washed with modified column buffer A, then proteins were eluted with a gradient of modified column buffer B, which is the same as the modified column buffer A with the addition of 1 M NaCl. The NaCl gradient was modified from Purification I: the first step was from 0-10%, the second step was from 10-56%, and the third step was from 56-100%.

Table 3: Summary of HLPFK Purification II.

Sample	Vol (mL)	Activity (U/mL)	Protein (mg/mL)	Specific Activity (U/mg)	Total Units (U)	Yield (%)	Purification Fold
Cleared Lysate	100	41	9.5	4.4	4220	100	1
Heat Denaturation	94	39	4.5	8.7	3650	86	2
$(NH_4)_2SO_4$ Precipitate	95	25	0.99	25	2350	56	6
HiQ	130	11	0.21	51	1350	32	12
Sepharose 2B	0.50	220	1.7	130	670	16	29

The elution profile is shown in Figure 9A. The black box indicates the pooled fractions (specific activity 51 U/mg), which were subsequently concentrated with 55% ammonium sulfate and then resuspended in about 2mL of gel buffer (20 mM KP_i pH 7.6, 3 mM $MgSO_4$, 5 mM DTT, 0.1 mM EDTA, 1 mM F6P) and applied to the same Sepharose 2B column. The elution profile for the gel filtration procedure is shown in Figure 9B. The pooled fractions (black box) had a specific activity of 130 U/mg. Purified protein was dialyzed into and then maintained in storage buffer (20 mM KP_i pH 7.6, 3 mM $MgSO_4$, 5

mM DTT, 0.1 mM EDTA, 1 mM F6P, and 20% glycerol (w/v)) for up to two months before decreased activity was observed, as in Purification I.

Purification II is summarized by Table 3 and Figure 10. Protein concentrations were determined using the Reducing Agent Compatible Pierce BCA Protein Assay Kit.

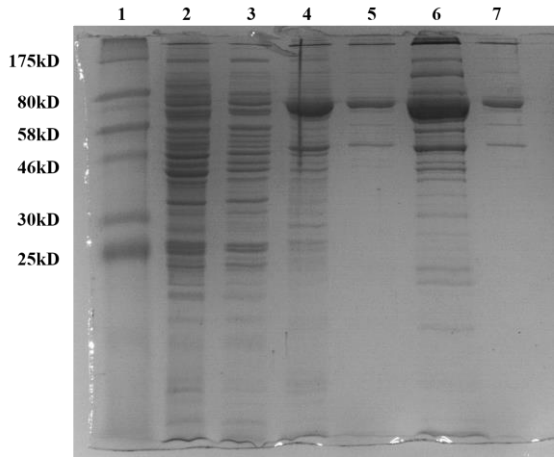

Figure 10: SDS-PAGE of Purification II. Lanes are (1) molecular weight marker, (2) cleared lysate, (3) heat denatured sample, (4) 33% ammonium sulfate pellet, (5) HiQ pool, (6) Sepharose 2B load, (7) pooled Sepharose 2B pool.

General Usage Guidelines for Purified Protein

HLPFK requires either MgATP or F6P to be present in storage conditions to remain active. The protein also requires DTT to be active. When measuring initial rates of HLPFK, it is important to allow the protein to incubate at room temperature for at least thirty min between initial dilution and kinetic measurements.

Comparison with Rat Liver Phosphofructokinase

Once HLPFK was purified, the first experiments examined the effects of the two substrates, F6P and MgATP. By measuring the $K_{1/2}$ for F6P at various concentrations of MgATP, the coupling free energy between F6P and MgATP was calculated. This analysis was repeated for RLPFK to compare the two enzymes. Purified RLPFK was obtained from David Holland. The data is shown in Figure 11 and the fit parameters from Equation 3 are listed in Table 4.

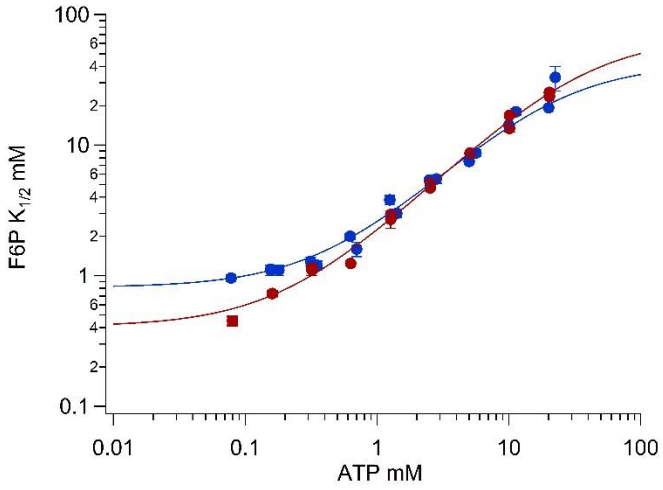

Figure 11: Comparison of HLPFK and RLPFK F6P and ATP binding at pH 7. Human liver PFK is represented by red, while rat liver PFK is represented by the blue. Both data sets were fit to Equation 3.

Table 4: Comparison of HLPFK and RLPFK at pH 7 at 25°C.

	K^0_{ia} (mM) (F6P)	K^0_{ix} (mM) (ATP)	Q_{ax}	ΔG_{ax}(kcal/mol)
HLPFK	0.41 ± 0.02	0.21 ± 0.01	0.0060 ± 0.004	3.0 ± 0.4
RLPFK	0.81 ± 0.3	0.43 ± 0.03	0.019 ± 0.002	2.3 ± 0.1

Graphically, we can see that HLPFK (red) and RLPFK (blue) have similar shapes. HLPFK binds F6P and MgATP tighter than RLPFK, as evidenced by the changes in the y-intercept (K_{ia}^{0}) and the beginning of the upward transition (K_{ix}^{0}), although the coupling free energy between F6P and MgATP is larger than RLPFK (as evidenced by the difference in the upper and lower plateau, Q_{ax}). With a difference in coupling free energy of 0.7 ± 0.4 kcal/mol, the coupling between F6P and MgATP is different for rat and human liver PFKs.

Effect of pH

During the purification, it was observed that HLPFK was easier to saturate with F6P at higher pH. The maximal velocity assay was conducted at pH 8.5 for HLPFK, although for RLPFK the assay was conducted at pH 8.[24] This observation led to the more systematic analysis of the effect of pH on the binding of F6P and MgATP shown in Figure 12 and Table 5. In the table, K_{ia}^{0} represents F6P binding in the absence of MgATP while K_{ix}^{0} represents MgATP binding in the absence of F6P.

As pH increases, HLPFK binds F6P more tightly, but MgATP binding doesn't change between pH 7 and 8. HLPFK binds MgATP tighter at pH 6 than at other pH values from the data. The coupling free energy between F6P and MgATP binding does not appear to be pH dependent, as ΔG_{ax} does not change over the range examined.

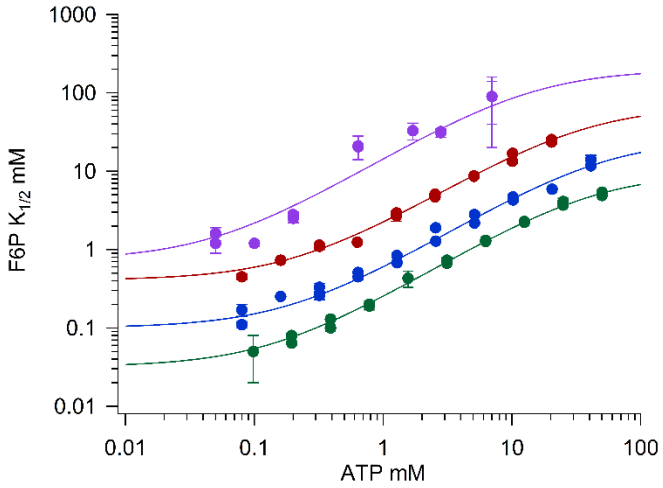

Figure 12: MgATP and pH Effect on F6P Binding. The purple data was measured at pH 6.0, the red data measured at pH 7.0, the blue data measured at pH 8.0, and the green data measured at pH 9.0.

Table 5: pH and MgATP Effect on F6P Binding at 25°C.

pH	K_{ia}^{0} (mM) (F6P)	K_{ix}^{0} (mM) (ATP)	Q_{ax}	ΔG_{ax}(kcal/mol)
6.0	0.70 ± 0.20	0.05 ± 0.01	0.0040 ± 0.0010	3.3 ± 0.2
7.0	0.41 ± 0.02	0.21 ± 0.01	0.0060 ± 0.0004	3.0 ± 0.1
8.0	0.100 ± 0.007	0.19 ± 0.01	0.0038 ± 0.0002	3.3 ± 0.1
9.0	0.032 ± 0.005	0.14 ± 0.02	0.0033 ± 0.0005	3.4 ± 0.1

Allosteric Effectors

After comparing the binding of F6P and MgATP between RLPFK and HLPFK and over the range of pH values, the next experiments sought to examine changes in HLPFK activity in the company of different allosteric effectors. The lower limit of 0.3 mM was chosen to eliminate the possibility of MgATP scarcity limiting the reaction rate.

The upper limit of 10 mM was chosen because at higher MgATP concentrations the $K_{1/2}$ for F6P becomes larger than can be reasonably measured.

Fructose-1,6-Bisphosphate

Fructose-1,6-bisphosphate is a product of the PFK reaction, which makes the investigation of the allosteric effect challenging. The coupling system described in Figure 3A works by removing F16BP as quickly as possible and is therefore not useful in investigating this ligand. An alternate coupling system utilizing pyruvate kinase and lactate dehydrogenase (Figure 3B) was used instead and the reaction was only allowed to produce 10 µM F16BP in order to accurately measure the initial rates.

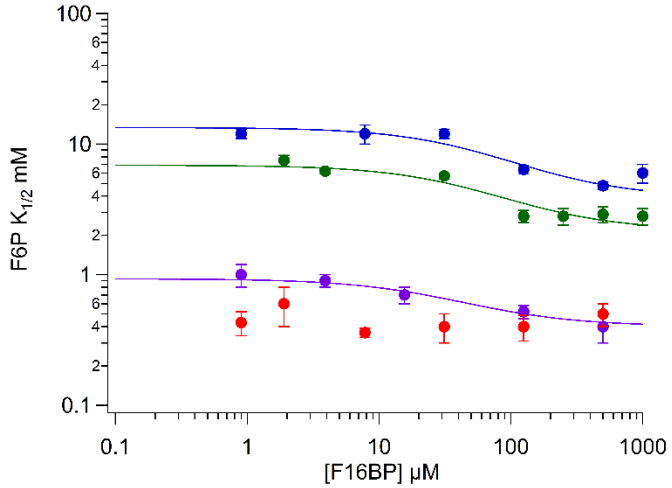

Figure 13: MgATP and F16BP Effect on F6P Binding. Blue data was collected with 10 mM MgATP present, green data was with 3 mM MgATP, purple data had 1 mM MgATP, and red data had 0. 3mM MgATP.

Figure 13 demonstrates the modest activation effect of F16BP on F6P binding at four MgATP concentrations, 0.3 mM (red), 1 mM (purple), 3 mM (green), and 10 mM

(blue) while Table 6 contains the parameters obtained from fitting the data to Equation 3. In the table, K_{ia}^{0} represents F6P binding in the absence of F16BP while K_{ix}^{0} represents F16BP binding in the absence of F6P. From the data, we can see that as MgATP decreases, HLPFK binds F6P and F16BP tighter. The coupling free energy does not change dramatically between 1 and 10 mM MgATP, although at 1 mM MgATP the coupling free energy is decreased and there does not appear to be any coupling between F6P and F16BP at 0.3 mM MgATP.

Table 6: F16BP and MgATP Effect on F6P Binding at 25°C.

MgATP (mM)	K_{ia}^{0} (mM) (F6P)	K_{ix}^{0} (µM) (F16BP)	Q_{ax}	ΔG_{ax}(kcal/mol)
10	13.4 ± 0.9	190 ± 90	3.4 ± 0.5	-0.72 ± 0.09
3	6.9 ± 0.3	160 ± 70	3.2 ± 0.5	-0.69 ± 0.09
1	0.93 ± 0.08	70 ± 80	2.3 ± 0.6	-0.49 ± 0.15
0.3	N/A	N/A	N/A	N/A

Adenosine Monophosphate

Adenosine monophosphate is a cellular indicator of low ATP that activates several PFKs and so it was selected as the next ligand in this study. Figure 14 contains the data from these experiments. The different colors represent the MgATP concentrations, 0.3 mM (red), 1 mM (purple), 3 mM (green), and 10 mM (blue). The data show a slight activation before AMP begins to act as an inhibitor. Unfortunately this behavior prevented fitting to Equation 3.

At low MgATP concentrations it appears that AMP begins inhibiting F6P binding around 2 mM. This inhibition is less dramatic at higher MgATP concentrations and appears to require higher AMP concentrations for the inhibitory effect (10 mM AMP at 10 mM MgATP). There is minimal activation observed at 10 mM MgATP with the other MgATP concentrations showing no coupling between F6P and AMP. This is especially interesting as AMP activates other mammalian PFKs (see discussion).

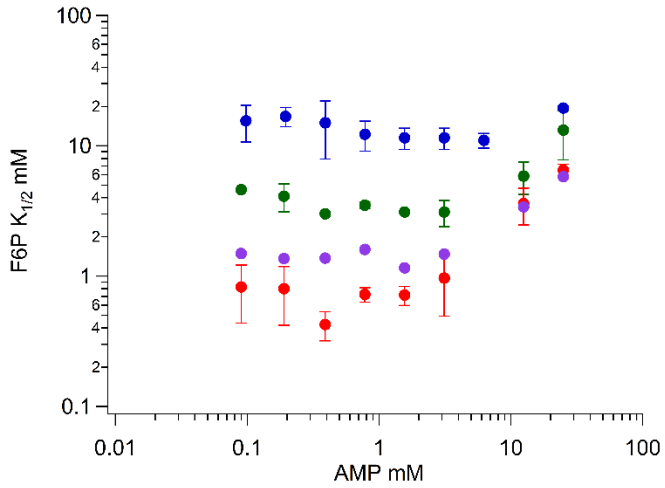

Figure 14: MgATP and AMP Effect on F6P Binding. Blue data was collected with 10 mM MgATP present, green data was with 3 mM MgATP, purple data had 1 mM MgATP, and red data had 0.3 mM MgATP.

Citrate

Citrate is an intermediate of the Krebs cycle, which occurs after glycolysis *in vivo*, which directly inhibits mammalian PFKs. The effect of citrate on HLPFK activity was examined as a function of F6P concentration at different MgATP concentrations. Figure

15 shows the results of those experiments and Table 6 summarizes the parameters obtained by fitting the data to Equation 3. In the table, K_{ia}^{0} represents F6P binding in the absence of citrate while K_{ix}^{0} represents citrate binding in the absence of F6P.

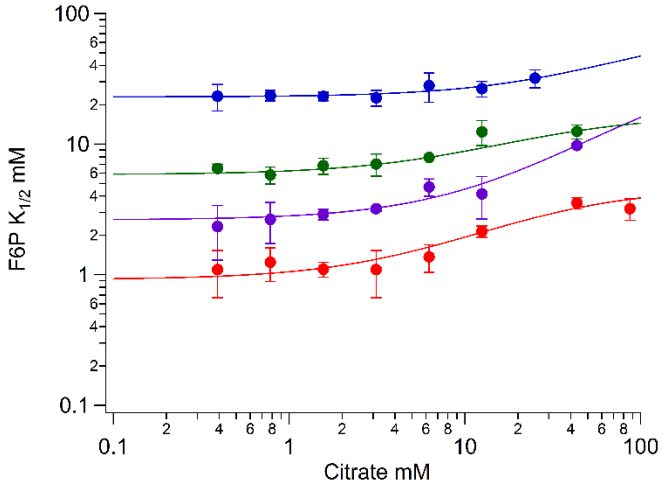

Figure 15: MgATP and Citrate Effect on F6P Binding. Blue data was collected with 10 mM MgATP present, green data was with 3 mM MgATP, purple data had 1 mM MgATP, and red data had 0.3 mM MgATP.

Table 7: Citrate and MgATP Effect on F6P Binding at 25°C.

MgATP (mM)	K_{ia}^{0} (mM) (F6P)	K_{ix}^{0} (mM) (citrate)	Q_{ax}	ΔG_{ax}(kcal/mol)
10	23.0 ± 0.6	40 ± 60	0.28 ± 0.66	0.75 ± 1.4
3	5.8 ± 0.3	9 ± 4	0.35 ± 0.10	0.62 ± 0.17
1	2.62 ± 0.09	12 ± 5	0.06 ± 0.07	1.7 ± 0.7
0.3	0.92 ± 0.06	5 ± 2	0.20 ± 0.04	0.95 ± 0.12

From these data, where the concentration of MgATP is 0.3 mM (red), 1mM (purple), 3 mM (green), or 10 mM (blue), it is apparent that the binding of citrate does not depend on MgATP concentration, as evidenced by a constant K_{ix}^{0}. The coupling free energy between citrate and F6P does not depend on the concentration of MgATP.

Ammonium Sulfate

After observing inconsistent data in early experiments that was eventually tracked to the preparation of coupling enzymes, the effect of ammonium sulfate on enzyme activity was examined. While not a physiological effector of HLPFK, many enzymes were supplied in ammonium sulfate suspensions and the effect on HLPFK is a technical consideration.

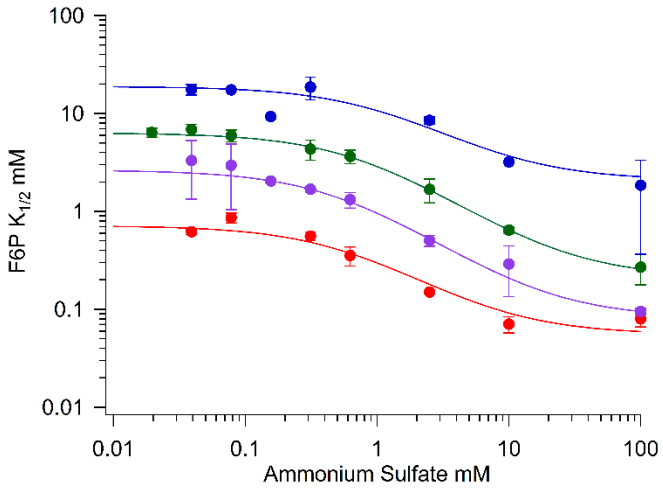

Figure 16: MgATP and Ammonium Sulfate Effect on F6P Binding. Blue data was collected with 10 mM MgATP present, green data was with 3 mM MgATP, purple data had 1 mM MgATP, and red data had 0.3 mM MgATP.

Table 8: Ammonium Sulfate and MgATP Effect on F6P Binding at 25°C.

MgATP (mM)	K_{ia}^{0} (mM) (F6P)	K_{ix}^{0} (mM) (ammonium sulfate)	Q_{ax}	ΔG_{ax}(kcal/mol)
10	19 ± 3	10 ± 20	10 ± 10	-1.4 ± 0.6
3	6.3 ± 0.4	20 ± 10	30 ± 10	-2.0 ± 0.2
1	2.62 ± 0.09	17 ± 3	32 ± 3	-2.0 ± 0.1
0.3	0.72 ± 0.05	8 ± 4	13 ± 3	-1.5 ± 0.1

Similar to the figures containing other allosteric effectors, Figure 16 shows the effect of ammonium sulfate on F6P binding at 0.3 mM MgATP (red), 1 mM MgATP (purple), 3 mM MgATP (green), and 10 mM MgATP (blue). Table 8 summarizes the fit parameters from Equation 3. In the table, K_{ia}^{0} represents F6P binding in the absence of ammonium sulfate while K_{ix}^{0} represents ammonium sulfate binding in the absence of F6P. There may be an effect on ammonium sulfate binding due to MgATP, but it is difficult to interpret with the errors reported. The coupling free energy between ammonium sulfate and F6P appears to remain constant at the MgATP concentrations examined, although it decreases somewhat at 0.3 mM MgATP.

CHAPTER IV

DISCUSSION AND CONCLUSIONS

Human liver phosphofructokinase is an important enzyme about which little has been published. Understanding the regulation of the first committed step of glycolysis in a cell that alternatively undergoes glycolysis and gluconeogenesis has implications for a variety of human diseases. Filling this gap in our knowledge begins with generating enzyme to study.

The first novelty of this work is the expression of HLPFK in an *E. coli* expression system. Utilizing the control of the *tac* promotor in pALTER-EX1 provided compatibility with the *tonA, pfka,* and *pfkb* deficient expression strain, RL257a. This strain was developed especially for expression of prokaryotic PFKs[52] and has proven useful in the expression of HLPFK, as shown in this work. Early preps had as few as 100 units per gram wet weight of cells in the crude lysate; Purification I is an example of this procedure and while it produced enough enzyme for some kinetics, the investigation in a better expression system was ongoing.

The addition of the optimized RBS improved expression by about five-fold, to about 450 units per gram wet weight of cells, and improved the purification. Increased expression provided the opportunity for more conservative pools to prioritize higher specific activity. The data presented as an example of Purification I were collected prior to the addition of the optimized RBS while Purification II data was collected using the new expression system.

Both protocols were adapted from the rat liver PFK procedure of Reinhart[24] with minor changes. The differences between Purification I and Purification II were also minor. Differences were related to buffer components; HLPFK was always stored in the presence of either ATP or F6P. One efficiency introduced into Purification II was the modification of the ammonium sulfate precipitation. Fractionating the heated supernatant (as in Purification I) was time consuming while the alternative buffer (containing ATP instead of F6P) allows HLPFK to precipitate at 33% ammonium sulfate. In Purification I, the first day of purification ends at the ammonium sulfate step, but following Purification II, the proteins can be eluted and concentrated from the anion exchange column in day one. The anion exchange step was somewhat modified between the purifications. While the MonoQ and HiQ resins differ in capacity, the buffer in Purification I has a higher ionic strength than that in Purification II. This likely leads to weaker interactions between the protein and resin in Purification II, evidenced by the later elution of HLFPK. Finally, Purification II yielded a higher purity sample (130 U/mg) than Purification I (105 U/mg).

The RLPFK procedure begins with rat livers[24] while the HLPFK procedure begins with *E. coli* cells. RLPFK purification begins with an ATP-containing buffer while HLPFK can be purified with either ATP- or F6P-containing buffer. The heat denaturation occurs at 55 ± 1°C for HLPFK while 60 ± 1°C was used for RLPFK. Both chromatographic procedures utilized anion exchange chromatography; the HLPFK protocol used a MonoQ or HiQ resin on a fast flow liquid chromatography system while the RLPFK procedure utilized a DEAE cellulose resin. Both purifications used the same gel filtration resin as a polishing step. HLPFK purified from a bacterial expression system

has a specific activity of 130 U/g while the RLPFK purified from the natural source was purified to 85 U/g.[24] Both proteins have a subunit molecular weight around 85000 Da as shown on SDS-PAGE gels.

After purification, the comparison of human and rat liver PFKs was conducted with respect to MgATP and F6P at pH 7. HLPFK and RLPFK are very similar, with 96% sequence similarity and 88% sequence identity. The RLPFK used in this experiment was obtained from David Holland, who purified the enzyme from a bacterial expression system similar to that developed in this work. From the data in Figure 11, both enzymes show a similar effect of MgATP on F6P binding. Based on the coupling free energy, RLPFK has a smaller coupling than HLPFK. In comparing these data to previously published RLPFK, Reinhart reported the coupling free energy between MgATP and F6P of RLPFK to be 1.87 kcal/mol.[58] These values differ from the values in this report, and some of that difference may be explained by the different origin of the sample. The L-type PFK isozyme is not the only type present in hepatocytes, and as Reinhart purified RLPFK from natural sources, it is possible that PFK-M and PFK-C isozymes were also present in the sample, which may have some effect on the activity. Binding of F6P and MgATP was tighter in Reinhart's purification (K_{ia}^0 0.171 mM and K_{ix}^0 0.31 mM)[24] than the expressed RLPFK while Reinhart's purification binds F6P tighter and MgATP less tightly than HLPFK. ATP inhibits HLPFK more that either RLPFK preparation and the recombinantly expressed RLPFK was more sensitive to inhibition by ATP than the RLPFK from natural sources as evidenced by the coupling free energies.

The effect of MgATP inhibition was next investigated over a range of pH values. The data at pH 6 were poorly behaved compared to those collected at higher pH values. The more favorable F6P binding at higher pH was previously documented in rat liver, when Reinhart examined the coupling between MgATP and F6P over the pH range from 5.5 to 9.[58] For both HLPFK and RLPFK the K_{ia}^{0} decreases as pH increases. The MgATP binding remains similar except at low pH for both enzymes. Binding sensitivity to pH changes generally indicates changing protonation state of the binding site, leading to changes in the allosteric effect. In PFKs from *E. coli* and *Bacillus stearothermophilus* important active site residues include aspartic acid, arginine, histidine, and serine,[59,60] all of which are affected by local pH. It seems likely that the F6P binding to HLPFK is dramatically influenced by the protonation states of active site residues. With regard to the coupling free energy of MgATP and F6P, it does not appear to be pH-dependent. It is interesting that the coupling between MgATP and F6P is not influenced by pH in HLFPK, as rabbit muscle PFK exhibits allostery over a range of pH values, but has no allosteric effects at pH 8.[61,62]

Despite being a product of the PFK reaction, F16BP activates HLPFK. The allosteric site for F16BP and F26BP has been suggested to evolve from a duplication event of the F6P site.[28] The activation of HLPFK by F16BP was modest and somewhat influenced by the concentration of MgATP. The coupling free energy between F6P and F16BP appears to decrease slightly at 1 mM MgATP and disappear at 0.3 mM MgATP. In comparing this trend to RLPFK data, both enzymes show activation behavior. Reinhart demonstrated activation for the F16BP range from 0-250 μM, with the $K_{1/2}$ changing

approximately five-fold.[24] The HLPFK effect is less than the RLPFK with only a two-fold change at 3 mM MgATP. The concentration of F16BP in hepatocytes has been reported as 20 μM,[22] a concentration that demonstrates limited activation alone for HLPFK. This suggests that some combination of ligands in necessary for activity under physiological conditions; F16BP does not activate sufficiently for cellular activity.

The next ligand studied was AMP, and it demonstrated the most unexpected data. AMP is well established as an activator of mammalian PFKs, including rat liver.[24,62] HLPFK showed minimal activation at 10mM MgATP and no activation at lower concentrations of MgATP. More surprisingly, inhibition was observed at higher concentrations of AMP, with the inhibitory behavior depending on the MgATP concentration. As the effects of AMP vary with MgATP concentration, it seems likely the bindings sites are linked in some way. In rabbit muscle PFK, this linkage has been demonstrated[32] and implicated in Tarui disease.[8] Hepatocytes contain approximately 0.3 mM AMP;[23] this study suggests that AMP is not sufficient to activate HLPFK *in vivo* and that the inhibition behavior observed may not have physiological relevance.

Citrate is a noted allosteric effector of mammalian PFKs and a downstream product of glycolysis that directly inhibits PFK. Citrate is present in hepatocytes at 0.2 mM, and Reinhart observed inhibition by citrate over the range from 0-5 mM.[24] This study examined citrate between 0 and 90 mM and little inhibition was observed. Citrate and MgATP have been suggested to synergistically inhibit the mammalian PFKs, but the inhibition effect of citrate was not influenced by MgATP concentration. Citrate and F6P binding do not appear to influence each other. Citrate has been suggested to couple the

Krebs cycle to glycolysis and produce the Warburg effect, rather than the Pasteur effect.[5] The Warburg effect is a marker of cancerous cells where a high rate of glycolysis is observed under aerobic conditions which stands in direct contrast to the Pasteur effect, where pyruvate is converted to acetyl CoA in the presence of oxygen in order to facilitate oxidative phosphorylation. The effect of citrate on HLPFK in combination with other ligands is one of the next areas of investigation.

The effect of ammonium sulfate was studied after it was determined that residual ammonium sulfate in the coupling enzyme preparation was affecting the repeatability of measurements. Additionally, activation by ammonia has been suggested as a method for increasing downstream formation of ATP and α-ketoglutarate, which are involved directly in ammonia fixation into glutamate and glutamine.[14] The concentration of ammonia in hepatocytes has been cited as 0.6 mM,[25] and this study examined the range from 0 to 100 mM. The coupling free energy between F6P and ammonia changes little over the MgATP concentration range, suggesting the effect is independent of MgATP.

Liver PFK has consistently proved a challenging enzyme to study. In this work, the variation of the F6P binding in the absence of second ligand (K_{ia}^{0}) in different experiments at the same MgATP concentration is telling. At 10 mM MgATP, the K_{ia}^{0} is about 15-20 mM while 3 mM MgATP presents a K_{ia}^{0} of about 6 mM. The K_{ia}^{0} at 1 mM MgATP is about 2 mM and at 0.3mM MgATP it is about 0.8 mM. These values were obtained with multiple enzyme preps, although the specific activity for all preps was in the range of 90-140 U/mg. The method of addition of MgATP and F6P to the reaction influenced the reproducibility of results. Assay cocktail and ligands were mixed prior to

the addition of enzyme, which began the measurements. The dependence on environment prior to assay may be related to the quaternary structure of the enzyme. As F6P favors higher order structures in RLPFK,[21] it seems possible the enzyme begins to dissociate to the tetramer upon the addition of MgATP, or vice versa. The sensitivity of HLPFK to ligands and protein concentration made measurements challenging.

The data presented herein represent the beginning of rigorous kinetic study of HLPFK. A successful growth and expression protocol was presented and initial kinetic characterizations are completed with the purified sample. These results suggest that the human liver enzyme is less sensitive to allosteric effectors than the rat liver enzyme, with the possible exception of MgATP. Future analyses will include the examination of F26BP effects and study on the oligomeric state of HLPFK in pursuit of the ultimate goal to determine how the enzyme functions in hepatocytes.

REFERENCES

(1) Hasawi, N. A., Alkandari, M. F., and Luqmani, Y. A. (2014) Phosphofructokinase: A mediator of glycolytic flux in cancer progression. *Crit. Rev. Oncol. Hematol. 92*, 312–321.

(2) López-Lázaro, M. (2008) The Warburg effect: why and how do cancer cells activate glycolysis in the presence of oxygen? *Anticancer. Agents Med. Chem. 8*, 305–312.

(3) Vijayakumar, S. N., Sethuraman, S., and Krishnan, U. M. (2015) Metabolic pathways in cancers: key targets and implications in cancer therapy. *R. Soc. Chem. Adv. 5*, 41751–41762.

(4) Zancan, P., Sola-Penna, M., Furtado, C. M., and Da Silva, D. (2010) Differential expression of phosphofructokinase-1 isoforms correlates with the glycolytic efficiency of breast cancer cells. *Mol. Genet. Metab. 100*, 372–378.

(5) Icard, P., and Lincet, H. (2012) A global view of the biochemical pathways involved in the regulation of the metabolism of cancer cells. *Biochim. Biophys. Acta 1826*, 423–433.

(6) Knobler, H., Weiss, Y., Peled, M., and Groner, Y. (1997) Impaired glucose-induced insulin response in transgenic mice overexpressing the L-phosphofructokinase gene. *Diabetes 46*, 1414–1418.

(7) Donofrio, J. C., Thompson, R. S., Reinhart, G. D., and Veneziale, C. M. (1984) Quantification of liver and kidney phosphofructokinase by radioimmunoassay in fed, starved and alloxan-diabetic rats. *Biochem. J. 224*, 541–7.

(8) Brüser, A., Kirchberger, J., and Schöneberg, T. (2012) Altered allosteric regulation

of muscle 6-phosphofructokinase causes Tarui disease. *Biochem. Biophys. Res. Commun. 427*, 133–7.

(9) Elson, A., Levanon, D., Weiss, Y., and Groner, Y. (1994) Overexpression of liver-type phosphofructokinase (PFKL) in transgenic-PFKL mice: implication for gene dosage in trisomy 21. *Biochem. J. 299*, 409–15.

(10) Elson, A., Bernstein, Y., Degani, H., Levanon, D., Ben-Hur, H., and Groner, Y. (1992) Gene dosage and Down's syndrome: Metabolic and enzymatic changes in PC12 cells overexpressing transfected human liver-type phosphofructokinase. *Somat. Cell Mol. Genet. 18*, 143–161.

(11) Vora, S., Seaman, C., Durham, S., and Piomelli, S. (1980) Isozymes of human phosphofructokinase: identification and subunit structural characterization of a new system. *Proc. Natl. Acad. Sci. U. S. A. 77*, 62–6.

(12) Kasten, T. P., Naqui, D., Kruep, D., and Dunaway, G. A. (1983) Purification of homogeneous rat phosphofructokinase isozymes with high specific activities. *Biochem. Biophys. Res. Commun. 111*, 462–469.

(13) González, F., Tsai, M. Y., and Kemp, R. G. (1975) Distribution of phosphofructokinase isozymes in rabbit, mouse, guinea pig and rat. *Comp. Biochem. Physiol. Part B Comp. Biochem. 52*, 315–319.

(14) Dunaway, G. A., and Weber, G. (1974) Rat liver phosphofructokinase isozymes. *Arch. Biochem. Biophys. 162*, 620–628.

(15) Dunaway, G. A., and Kasten, T. P. (1987) Nature of the subunits of the 6-phosphofructo-1-kinase isoenzymes from rat tissues. *Biochem. J. 242*, 667–671.

(16) Dunaway, G. A., Kasten, T. P., Sebo, T., and Trapp, R. (1988) Analysis of the phosphofructokinase subunits and isoenzymes in human tissues. *Biochem. J. 251*, 677–83.

(17) Reinhart, G. D., and Lardy, H. A. (1980) Rat liver phosphofructokinase: use of fluorescence polarization to study aggregation at low protein concentration. *Biochemistry 19*, 1484–90.

(18) Zancan, P., Marinho-Carvalho, M. M., Faber-Barata, J., Dellias, J. M. M., and Sola-Penna, M. (2008) ATP and fructose-2,6-bisphosphate regulate skeletal muscle 6-phosphofructo-1-kinase by altering its quaternary structure. *IUBMB Life 60*, 526–33.

(19) Reinhart, G. D., and Hartleip, S. B. (1987) Perturbation of the quaternary structure and allosteric behavior of rat liver phosphofructokinase by polyethylene glycol. *Arch. Biochem. Biophys. 258*, 65–76.

(20) Reinhart, G. D., and Lardy, H. A. (1980) Rat Liver Phosphofructokinase: Kinetic and physiological ramifications. *Biochemistry 19*, 1491–1495.

(21) Ranjit, S., Dvornikov, A., Holland, D. A., Reinhart, G. D., Jameson, D. M., and Gratton, E. (2014) Application of three-photon excitation FCS to the study of protein oligomerization. *J. Phys. Chem. B 118*, 14627–31.

(22) Furuya, E., and Uyeda, K. (1980) An activation factor of liver phosphofructokinase. *Proc. Natl. Acad. Sci. U. S. A. 77*, 5861–5864.

(23) Veech, R. L., Lawson, J. W., Cornell, N. W., and Krebs, H. A. (1979) Cytosolic phosphorylation potential. *J. Biol. Chem. 254*, 6538–6547.

(24) Reinhart, G. D., and Lardy, H. A. (1980) Rat liver phosphofructokinase: kinetic

activity under near-physiological conditions. *Biochemistry 19*, 1477–1484.

(25) Verhoeven, A. J., van Iwaarden, J. F., Joseph, S. K., and Meijer, A. J. (1983) Control of rat-liver glutaminase by ammonia and pH. *Eur. J. Biochem. 133*, 241–244.

(26) Ling, K., Marcus, F., and Lardy, H.A. (1965) Purification and some properties of rabbit skeletal muscle phosphofructokinase. *J. Biol. Chem. 240*, 1893–1899.

(27) Uyeda, K. (1979) Phosphofructokinase. *Adv. Enzymol. Relat. Areas Mol. Biol. 48*, 193–244.

(28) Schöneberg, T., Kloos, M., Brüser, A., Kirchberger, J., and Sträter, N. (2013) Structure and allosteric regulation of eukaryotic 6-phosphofructokinases. *Biol. Chem. 394*, 977–93.

(29) Sola-Penna, M., Da Silva, D., Coelho, W. S., Marinho-Carvalho, M. M., and Zancan, P. (2010) Regulation of mammalian muscle type 6-phosphofructo-1-kinase and its implication for the control of the metabolism. *IUBMB Life 62*, 791–6.

(30) Sharma, P. M., Reddy, G. R., Vora, S., Babior, B. M., and McLachlan, A. (1989) Cloning and expression of a human muscle phosphofructokinase cDNA. *Gene 77*, 177–83.

(31) Johnson, J. L., Raney, A. K., and Babior, B. M. (1992) Cloning and characterization of the human muscle phosphofructokinase gene. *DNA Cell Biol. 11*, 461–470.

(32) Brüser, A., Kirchberger, J., Kloos, M., Sträter, N., and Schöneberg, T. (2012) Functional linkage of adenine nucleotide binding sites in mammalian muscle 6-phosphofructokinase. *J. Biol. Chem. 287*, 17546–53.

(33) Bosca, L., Aragon, J. J., and Sols, A. (1985) Modulation of muscle

phosphofructokinase at physiological concentration of enzyme. *J. Biol. Chem. 260*, 2100–2107.

(34) Hers, H., and Van Schaftingen, E. (1982) Fructose 2,6-bisphosphate 2 years after its discovery. *Biochem. J. 206*, 1–12.

(35) Claus, T. H., Schlumpf, J. R., El-Maghrabi, M. R., Pilkis, J., and Pilkis, S. J. (1980) Mechanism of action of glucagon on hepatocyte phosphofructokinase activity. *Proc. Natl. Acad. Sci. U. S. A. 77*, 6501–5.

(36) Van Schaftingen, E., Jett, M. F., Hue, L., and Hers, H. G. (1981) Control of liver 6-phosphofructokinase by fructose 2,6-bisphosphate and other effectors. *Proc. Natl. Acad. Sci. U. S. A. 78*, 3483–6.

(37) Bartrons, R., Hue, L., Van Schaftingen, E., and Hers, H. (1983) Hormonal control of fructose 2 ,6-bisphosphate concentration in isolated rat hepatocytes. *Biochem. J. 214*, 829–837.

(38) Schliselfeld, L. H., and Danon, M. J. (1996) Use of fructose-2,6-diphosphate to assay for phosphofructokinase activity in human muscle. *Clin. Biochem. 29*, 79–83.

(39) Reinhart, G. D. (1983) Influence of fructose 2,6-bisphosphate on the aggregation properties of rat liver phosphofructokinase. *J. Biol. Chem. 258*, 10827–10830.

(40) Uyeda, K., Furuya, E., and Luby, L. J. (1981) The effect of natural and synthetic D-fructose 2,6-bisphosphate on the regulatory kinetic properties of liver and muscle phosphofructokinases. *J. Biol. Chem. 256*, 8394–9.

(41) Reinhart, G. D., and Hartleip, S. B. (1992) Influence of fructose 2,6-bisphosphate and MgATP on rat liver phosphofructokinase at pH 7: Evidence for a complex

interdependence. *Arch. Biochem. Biophys. 296*, 224–30.

(42) Pilkis, S. J., El-Maghrabi, M. R., Pilkis, J., Claus, T. H., and Cumming, D. A. (1981) Fructose 2,6-bisphosphate: A new activator of phosphofructokinase. *J. Biol. Chem. 256*, 3171–3174.

(43) Arechaga, I., Martínez-Costa, O. H., Ferreras, C., Carrascosa, J. L., and Aragón, J. J. (2010) Electron microscopy analysis of mammalian phosphofructokinase reveals an unusual 3-dimensional structure with significant implications for enzyme function. *FASEB J. 24*, 4960–8.

(44) Banaszak, K., Mechin, I., Obmolova, G., Oldham, M., Chang, S. H., Ruiz, T., Radermacher, M., Kopperschläger, G., and Rypniewski, W. (2011) The crystal structures of eukaryotic phosphofructokinases from baker's yeast and rabbit skeletal muscle. *J. Mol. Biol. 407*, 284–97.

(45) Kloos, M., Brüser, A., Kirchberger, J., Schöneberg, T., and Sträter, N. (2014) Crystallization and preliminary crystallographic analysis of human muscle phosphofructokinase, the main regulator of glycolysis. *Acta Crystallogr. Sect. F, Struct. Biol. Commun. 70*, 578–82.

(46) Kloos, M., Bruser, A., Kirchberger, J., Schoneberg, T., and Stater, N. (2015) Crystal structure of human platelet phosphofructokinase-1 locked in an activated conformation. *Biochem. J. 469*, 421–432.

(47) Webb, B. A., Forouhar, F., Szu, F.-E., Seetharaman, J., Tong, L., and Barber, D. L. (2015) Structures of human phosphofructokinase-1 and atomic basis of cancer-associated mutations. *Nature 523*, 111–114.

(48) Kono, N., Uyeda, K., and Oliver, R. M. (1973) Chicken liver phosphofructokinase: I. Crystallization and physicochemical properties. *J. Biol. Chem. 248*, 8592–8602.

(49) Reinhart, G. D. (1980) Influence of polyethylene glycols on the kinetics of rat liver phosphofructokinase. *J. Biol. Chem. 255*, 10576–10578.

(50) Vora, S., and Francke, U. (1981) Assignment of the human gene for liver-type 6-phosphofructokinase isozyme (PFKL) to chromosome 21 by using somatic cell hybrids and monoclonal anti-L antibody. *Proc. Natl. Acad. Sci. U. S. A. 78*, 3738–42.

(51) Levanon, D., Danciger, E., Dafni, N., Bernstein, Y., Elson, A., Moens, W., Brandeis, M., and Groner, Y. (1989) The primary structure of human liver type phosphofructokinase and its comparison with other types of PFK. *DNA 8*, 733–43.

(52) Lovingshimer, M. R., Siegele, D., and Reinhart, G. D. (2006) Construction of an inducible, pfkA and pfkB deficient strain of *Escherichia coli* for the expression and purification of phosphofructokinase from bacterial sources. *Protein Expr. Purif. 46*, 475–82.

(53) Weber, G. (1972) Ligand binding and internal equilibria in proteins. *Biochemistry 11*, 864–878.

(54) Reinhart, G. D. (1983) The determination of thermodynamic allosteric parameters of an enzyme undergoing steady-state turnover. *Arch. Biochem. Biophys. 224*, 389–401.

(55) Reinhart, G. D. (2004) Quantitative analysis and interpretation of allosteric behavior. *Methods Enzymol. 380*, 187–203.

(56) Reinhart, G. D. (1988) Linked-function origins of cooperativity in a symmetrical dimer. *Biophys. Chem. 30*, 159–72.

(57) Vellanoweth, R. L., and Rabinowitz, J. C. (1992) The influence of ribosome-binding-site elements on translational efficiency in *Bacillus subtilis* and *Escherichia coli in vivo*. *Mol. Microbiol. 6*, 1105–1114.

(58) Reinhart, G. D. (1985) Influence of pH on the regulatory kinetics of rat liver phosphofructokinase: A thermodynamic linked-function analysis. *Biochemistry 24*, 7166–72.

(59) Hellinga, H. W., and Evans, P. R. (1987) Mutations in the active site of *Escherichia coli* phosphofructokinase. *Nature 327*, 437–439.

(60) Shirakihara, Y., and Evans, P. R. (1988) Crystal structure of the complex of phosphofructokinase from *Escherichia coli* with its reaction products. *J. Mol. Biol. 204*, 973–994.

(61) Frieden, C., Gilbert, H. R., and Bock, P. E. (1976) Phosphofructokinase III. Correlation of the regulatory kinetic and molecular properties of the rabbit muscle enzyme. *J. Biol. Chem. 251*, 5644–5647.

(62) Kemp, R. G., and Foe, L. G. (1983) Allosteric regulatory properties of muscle phosphofructokinase. *Mol. Cell. Biochem. 57*, 147–154.